Ann Sci For (1995) 52, 23-42

Original article

Measurement and modelling of radiation transmission within a stand of maritime pine (*Pinus pinaster* Ait)

P Berbigier, JM Bonnefond

INRA, Laboratoire de Bioclimatologie, Domaine de la Grande-Ferrade, BP 81, 33883 Villenave-d'Ornon cedex, France

(Received 18 October 1993; accepted 13 June 1994)

Summary — A semi-empirical model of radiation penetration in a maritime pine canopy was developed so that mean solar (and net) radiation absorption by crowns and understorey could be estimated from above-canopy measurements only. Beam radiation R_b was assumed to penetrate the canopy according to Beer's law with an extinction coefficient of 0.32; this figure was found using non-linear regression techniques. For diffuse sky radiation, Beer's law was integrated over the sky vault assuming a SOC (standard overcast sky) luminance model; the upward and downward scattered radiative fluxes were obtained using the Kubelka–Munk equations and measurements of needle transmittance and reflectance. The penetration of net radiation within the canopy was also modelled. The model predicts the measured albedo of the stand very well. The estimation of solar radiation transmitted by the canopy was also satisfactory with the maximum difference between this and the mean output of mobile sensors at ground level being only 18 W m^{-2}. Due to the poor precision of net radiometers, the net radiation model could not be tested critically. However, as the modelled longwave radiation balance under the canopy is always between –10 and –20 Wm^{-2}, the below-canopy net radiation must be very close to the solar radiation balance.

model / solar radiation / net radiation / penetration / maritime pine

Résumé — Mesure et modélisation de la transmission du rayonnement à l'intérieur d'une parcelle de pins maritimes (*Pinus pinaster* Ait). *Un modèle semi-empirique de pénétration du rayonnement dans un couvert de pins maritimes a été établi, dans le but d'estimer l'absorption moyenne du rayonnement solaire et du rayonnement net par les houppiers et le sous-bois à partir des seules mesures faites au-dessus du couvert. Le rayonnement direct est supposé le pénétrer selon la loi de Beer, avec un coefficient d'extinction de 0,32 ; cette valeur a été obtenue par des techniques de régression non-linéaires. Pour le rayonnement diffus du ciel, cette loi a été intégrée sur toute la voûte céleste ; en supposant un modèle SOC* (standard overcast sky) *de luminance : les rayonnements rediffusés vers le haut et vers le bas sont obtenus au moyen des équations de Kubelka-Munk, avec des valeurs mesurées de la transmittance et de la réflectance des aiguilles. La pénétration du rayonnement net est*

aussi modélisée. Le modèle prédit très bien l'albedo mesurée de la parcelle. L'estimation du rayonnement solaire transmis par la canopée est elle aussi satisfaisante, la différence avec la réponse moyenne de capteurs mobiles au niveau du sol n'excédant pas 18 Wm^{-2}. La faible précision des pyrradiomètres ne permet pas de valider le modèle de rayonnement net : cependant, comme le bilan de grande longueur d'onde fourni par le modèle sous la canopée est faible (–10 à –20 Wm^{-2}), le rayonnement net sous la canopée doit être très proche du bilan du rayonnement solaire.

modèle / rayonnement solaire / rayonnement net / pénétration / pin maritime

INTRODUCTION

Evaporation and photosynthesis are closely related to the absorption of net radiation and the photosynthetically active radiation (PAR) by foliage elements. Thus, the development of a multi-layer description of canopy water and CO_2 exchange first demands that we model the absorption of net radiation and PAR by each layer.

The maritime pine forest of south-west France (Les Landes) consists of 2 well-separated foliage layers, the tree crowns and the understorey. It has been shown (Diawara, 1990) that the trunks have almost no effect on heat and mass exchange. The leaf area index (LAI) of the trees is low (~ 3), allowing a thick vegetal layer to develop at ground level, consisting of either *Gramineae* (wet areas) or bracken (dry areas). As the transpiration of the understorey may contribute to half of the total evaporation (Diawara, 1990; Diawara *et al,* 1991), it is important to estimate the proportion of radiation absorbed by each layer if we are to fully understand the hydrology of the forest.

The first micrometeorogical studies on Les Landes were performed during the Hapex–Mobilhy experiment in the summer of 1986 (Gash *et al,* 1989; Granier *et al,* 1990). Further work has attempted to quantify individual contributions to the total evaporation of the trees and understorey (Loustau *et al,* 1990; Berbigier *et al,* 1991; Diawara *et al,* 1991; Loustau and Cochard, 1991). However, radiation was poorly taken into account in these studies. In 1991, Bonnefond (1993) developed a mobile system integrating the measurements over a 22 x 4 m^2 area between 2 tree rows, in order to provide a better experimental foundation for the models of radiation penetration. Some results for solar radiation have already been published (Berbigier, 1993).

This paper will focus on solar and net radiation. As the detailed geometrical structure of the tree crowns is largely unknown, the model presented here is a semi-empirical one, which treats the canopy as a homogeneous turbid layer. While a discrete canopy model would in principal be more realistic for radiation, convective exchange can only be treated for horizontally continuous canopies. Since, to a good first approximation, canopy evaporation is proportional to the absorbed net radiation (Berbigier *et al,* 1991), such a level of sophistication seems unnecessary for estimating the energy balance.

No account is made for the clumping of pine needles. However, since the maritime pine shoots are widely spread, this effect must be less significant than for some other resinous species.

MATERIALS AND METHODS

Site

The experiment took place during the summers of 1991, 1992 and 1993, in a maritime pine stand aged about 20 years, 15–16 m high and situated 20 km from Bordeaux (latitude 44° 42'N, longitude 0° 46' W). The inter-row distance was 4 m.

After thinning in autumn 1990, the stand density was 660 trees per hectare. Rows were aligned along a NE–SW axis. Understorey comprised mainly *Gramineae* species about 0.7 m high. These remained green and turgid throughout the expriments.

Radiation measurements

Radiation sensors were mounted above the canopy from a 25 m high scaffolding. Two thermopiles (Cimel CE180), 1 facing upward and the other downward, measured incident and reflected global radiation. Net radiation was measured with a Didcot DRN/301 net radiometer.

At ground level, 5 radiation sensors were mounted on a 4-m-long transverse rod fixed on an electric trolley running on a 22 m railway secured 1 m above the ground. These sensors were Cimel thermopiles in 1991, net radiometers (Crouzet, INRA licence) in 1992, and both in 1993. More details can be found in Bonnefond (1993). For the most part, the data were averaged over 60 min.

In 1993, a thermophile with a shadow band mounted at 2 m above ground provided measurements of the incident diffuse radiation under the tree canopy. During a few days in late August–early September 1993 (day of the year [DOY] 242-243-244), a third Cimel thermopile mounted at the top of the scaffolding and equipped with a shadow band enabled us to estimate the local diffuse radiation; otherwise, this measurement was taken from Bordeaux.

Thermopiles were calibrated against a recently calibrated CM6, Kipp and Zonen thermopile, and net radiometers against a recently calibrated Rebs Q6 net radiometer. Despite this, the calibration coefficient of the Didcot net radiometer was obviously overestimated. The limited accuracy of net radiometers due to variations of the calibration coefficient with time, climate, sun elevation, side of the plate, characteristics of the plastic domes, wavelength, *etc*, has been widely discussed (Field *et al*, 1992; Halldin and Lindroth, 1992). Four separate calibration coefficients are involved, 2 for each side of the plate, 1 for solar radiation and the other for longwave radiation. However, as it is impossible to separate the individual effects of the 4 radiative components of the net radiometer, only one coefficient is used; this should at least be determined *in situ*, so that the ratio of the different radiation components is more or less the same as for measurements. This is particularly important for the Didcot instrument, which has thick semi-rigid domes which absorb and emit a significant amount of thermal radiation.

For the above reasons, in September 1993 an Eppley PIR pyrgeometer was mounted on top of the scaffolding, in order to correct the Didcot calibration with separate measurements of solar incident and reflected radiation as well as thermal infrared radiation from the sky and thermal emission of the canopy. The latter was estimated by means of Wien's law using canopy air temperature as a substitute for surface temperature, since they differ by no more than 1 degree (Diawara, 1990). This same correction was used for the 1992 data.

In 1991, 5 clear days (DOY 217-218-222-223-224), 1 overcast day (219) and 2 partially cloudy days (220-221); in 1992, 4 clear days (DOY 237-238-240-246) and 1 partially cloudy day (239); and in 1993, 5 clear days (DOY 177-178-242-243-244) and 1 overcast day (168) were chosen for analysis. In 1992, more days were available, but unfortunately the air temperature measurements necessary for net radiation modelling were not made.

Since the instruments were rarely all available at the same time, we were able to validate separately the models for direct and diffuse radiation from *in situ* measurements on only a few clear days (in 1993, DOY 242-243-244). However, for adjusting them, we chose the clear days 177 and 178 in 1993, even though the sky diffuse radiation was not measured on site, because, at this time of the year, changes in sun elevation are maximal allowing better precision of the adjustments. On clear days, the measurement of diffuse radiation at Bordeaux instead of on site induces a negligible error. Days 242, 243 and 244 were used for a validation as an independent set of data. The models were then compared with data of years 1991 and 1992.

Optical properties of the needles

The spectral reflectance and transmittance of the needles were determined using an integrating sphere (Licor, LI-1800) scanning the bandwidth from 400 to 1 100 nm. The sample port was 10 mm in diameter so that it could not be covered by a conifer needle. We followed the technique developed by Daughtry *et al* (1989). Briefly, this

consists of laying needles side by side approximately a needle-width apart and taping their extremities and measuring spectral transmission and reflection of this sample. The needles are then coated with an opaque flat black paint, and the transmittance of the blackened sample, *ie* the effect of gaps, is measured, taking care to lay the sample in the sample port in exactly the same position as before. It is then easy to account for the effect of the gaps and calculate the true spectral reflection and transmission coefficients of the needles.

Five samples of each age of needles (1, 2, 3 years) were analyzed. As the new season shoots had not yet opened at the time of measurements, they were not taken into account. The difference between 1, 2 and 3 year needles was non-significant, and so the average of 15 samples was finally retained.

The mean reflectance and transmittance over a given waveband were then calculated by summing the product of spectral reflectance and transmittance, respectively, by the spectral density of the incident beam radiation of a clear day, and dividing this sum by the sum of the spectral densities.

Leaf area index

The LAI of the stand was measured at regular intervals by an optical method based on the interception of the solar beam (Demon system, CSIRO, Australia: Lang, 1987).

THEORY

The penetration of the different radiative components in the canopy is schematized in figure 1.

Beam penetration

The non-intercepted direct beam radiation $R_b(\lambda)$ (W m^{-2}) at depth λ (cumulated LAI from the top of the canopy) can be written as:

$$R_b(\lambda) = R_b(0) \exp(-\kappa\lambda / \sin\beta) \qquad [1]$$

where $R_b(0)$ is the beam radiation above the canopy, β is the angular sun elevation, and κ is the extinction coefficient. For a spherical distribution of needles, κ takes the value of 0.5; otherwise, it varies with solar elevation (Sinoquet and Andrieu, 1993).

Diffuse radiation penetration

The penetration of the non-intercepted sky diffuse radiation is modelled in the following way. First, we assume that the diffuse flux originating from a given point of the sky vault penetrates the canopy according to equation [1] where β is the angular elevation of the source. In addition, we need to know how the diffuse luminance of the sky varies over the hemisphere. For this we use the standard overcast sky (SOC) law proposed by Steven and Unsworth (1980):

$$N(\beta) = \{N(\pi/2)/2.23\}\{1 + 1.23 \sin\beta\} \qquad [2]$$

where $N(\beta)$ is the luminance, assumed constant for any azimuth, of a ring of angular elevation β; $N(\pi/2)$ is the luminance of the zenith. Strictly speaking, this law is only true for overcast skies. For clear skies, the luminance may be described as the superposition of a background and a circumsolar term (Steven and Unsworth, 1979). Furthermore and contrary to the SOC model, the background luminance tends to decrease as the angular elevation increases. However, for clear skies, the diffuse flux density is less than 20% of the global radiation and so the relative error remains low. Moreover, the more cloudy the sky, the more accurate equation [2] becomes.

The mean flux density of diffuse radiation above the canopy may be written as:

$$R_d(0) = \{2\pi N(\pi/2)/2.23\} \int_0^1 (1 + 1.23u)u\,du$$
$$= 0.91\{2\pi N(\pi/2)/2.23\} \qquad [3a]$$

where $u = \sin\beta$

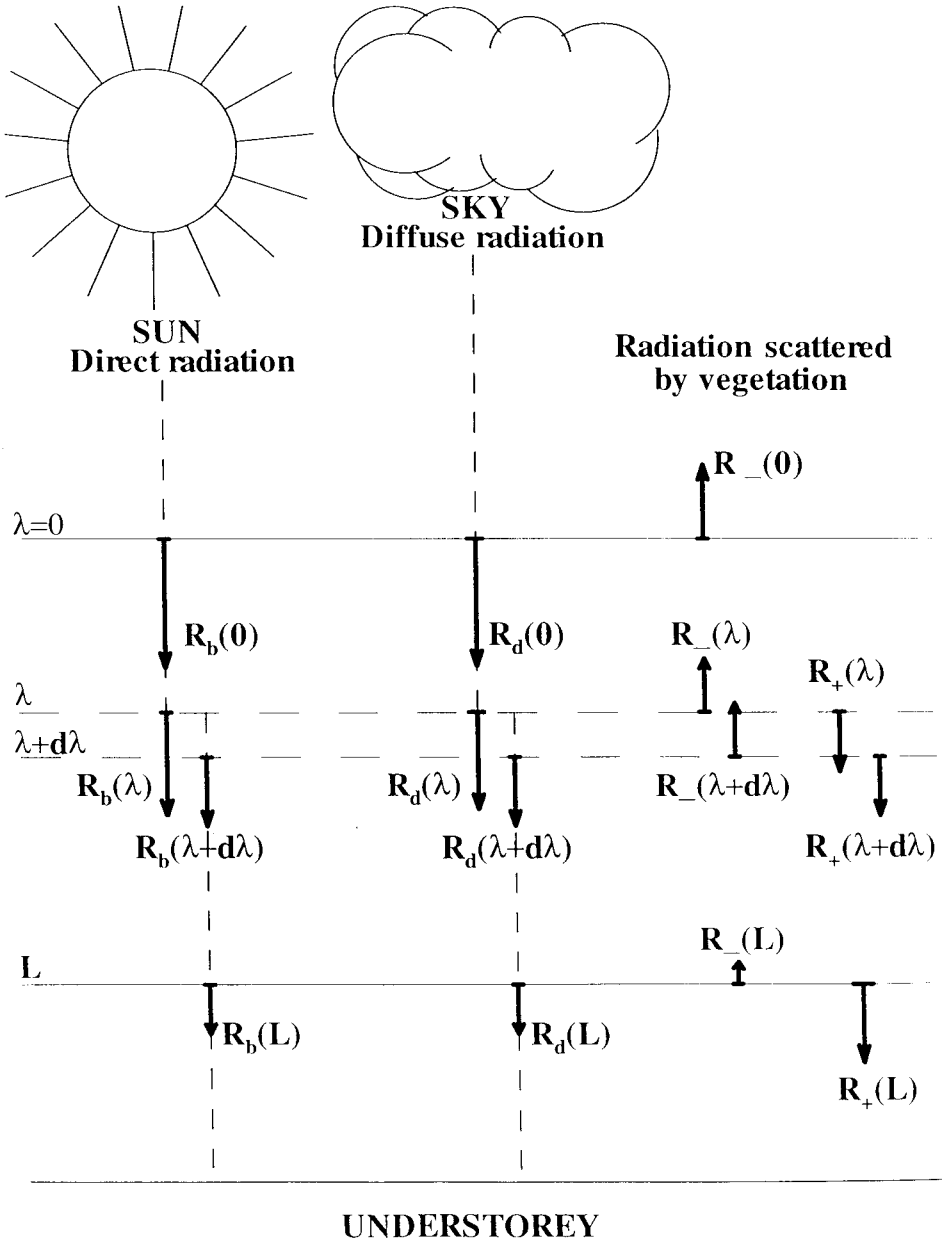

Fig 1. Schematic representation of direct (R_b) and sky diffuse radiation (R_d) which are not intercepted by the canopy, and downward (R_+) and upward (R_-) radiation rediffused by vegetation elements at different depths into the canopy defined by their cumulated LAI (λ). $\lambda = 0$: canopy top, $\lambda = L$: canopy bottom.

At level λ inside the canopy, the non-intercepted diffuse flux density is:

$$R_d(\lambda) = \{2\pi N(\pi/2)/2.23\} \int_0^1 \exp(-\kappa\lambda/u)\,(1 + 1.23u)\,u\,du \quad [3b]$$

so that:

$$R_d(\lambda) = \{R_d(0)/0.91\} \int_0^1 \exp(-\kappa\lambda/u)\,(1 + 1.23u)\,u\,du \quad [3c]$$

The ratio $R_d(\lambda)/R_d(0)$ can be approximated by the function $Y = \exp(-k'\lambda)$, with $k' = 0.467$, with maximum absolute error of 0.025 ($0 < \text{LAI} < 7$).

Rediffusion of the intercepted radiation

The method is based on the radiative balance of a thin canopy layer, following concepts given in Bonhomme and Varlet-Grancher (1977) and Sinoquet *et al* (1993). The main assumptions are: (a) that there is a random distribution of needle azimuth; (b) that the same distribution of inclination angles exists for all layers; (c) that there is no clumping of needles; (d) that the scattered radiation (upward and downward) is isotropic at each level of the canopy; and (d) that $R_d(\lambda)/R_d(0)$ can be described by a negative exponential of LAI.

The latter approximation allows us to find an analytical solution to the problem (Kubelka–Munk equations). A further assumption is usually made in that leaf reflectance ρ equals transmittance τ. For conifer needles, this hypothesis is unrealistic and here we will use the experimental values of ρ and τ obtained in the manner described above.

When a foliage element intercepts a beam of radiation, it reflects part of it and transmits another part. The canopy is divided into horizontal layers of equal thickness $d\lambda$ (*ie* equal proportions of LAI). Let $R_+(\lambda)$ be the downward rescattered flux density at level λ, $dR_1(\lambda)$ the part of $R_+(\lambda)$ that is intercepted by the i th layer situated at level λ, and k_i the interception coefficient of the i th layer. Then:

$$dR_1(\lambda) = -R_+(\lambda)\, k_i(\lambda)\, d\lambda$$

The value of k_i is always very close to 1 (Bonhomme and Varlet-Grancher, 1977) and with this approximation, the radiation balance at level λ can be written as:

$$dR_+(\lambda)/d\lambda = -(1-\tau)R_+(\lambda) + \rho R_-(\lambda) + \tau\{kR_b(\lambda) + k'R_d(\lambda)\} \quad [4a]$$

$$dR_-(\lambda)/d\lambda = (1-\tau)R_-(\lambda) - \rho R_+(\lambda) - \rho\{kR_b(\lambda) + k'R_d(\lambda)\} \quad [4b]$$

where $R_+(\lambda)$ is the downward rescattered radiation, $R_-(\lambda)$ is the upward rescattered radiation, $k = \kappa/\sin\beta$, k' is the extinction coefficient of diffuse radiation (assuming $R_d(\lambda)/R_d(0) = \exp(-k'\lambda)$), and ρ and τ are the reflectance and transmittance of the needles.

Rearranging [4a] and [4b] leads to the following 2nd-order linear differential equations:

$$d^2R_+(\lambda)/d\lambda^2 + \{\rho^2 - (1-\tau^2)\}R_+(\lambda) = -k\{(1-\tau)\tau + \rho^2 + k\tau\}R_b(0)e^{-k\lambda} - k'\{(1-\tau)\tau + \rho^2 + k'\tau\}R_d(0)e^{-k'\lambda} \quad [5a]$$

$$d^2R_-(\lambda)/d\lambda^2 + \{\rho^2 - (1-\tau^2)\}R_-(\lambda) = \rho k(k-1)R_b(0)e^{-k\lambda} + \rho k'(k'-1)R_d(0)e^{-k'\lambda} \quad [5b]$$

The equations have an analytical solution (Kubelka and Munk, 1931) which can be found in Bonhomme and Varlet-Grancher (1977) for the case of equal needle transmittance and absorptance. The solution presented below (equations [6] and [7]) is slightly more sophisticated.

$$R_+(\lambda) = C_1 e^{\alpha\lambda} + C_2 e^{-\alpha\lambda} + Q_1 R_b(0) e^{-k\lambda} + Q_2 R_d(0) e^{-k'\lambda} \quad [6a]$$

$$R_-(\lambda) = C_3 e^{\alpha\lambda} + C_4 e^{-\alpha\lambda} + Q_3 R_b(0) e^{-k\lambda} + Q_4 R_d(0) e^{-k'\lambda} \quad [6b]$$

where α is the albedo of the understorey, λ is the accumulated LAI of the canopy and

$$\alpha = \{(1-\tau)^2 - \rho^2\}^{0.5}$$
$$\beta = (-\alpha + \rho + 1 - \tau) / (\alpha + \rho + 1 - \tau) \quad [7a]$$

$$Q_1 = -k\{(1-\tau)\tau + \rho^2 + k\tau\}/(k^2 - \alpha^2) \quad [7b]$$

$$Q_2 = -k'\{(1-\tau)\tau + \rho^2 + k'\tau\}/(k'^2 - \alpha^2) \quad [7c]$$

$$Q_3 = \rho k (k-1)/(k^2 - \alpha^2) \quad [7d]$$

$$Q_4 = \rho k' (k'-1)/(k'^2 - \alpha^2) \quad [7e]$$

$$C_1 = \{e^{-\alpha L}[Q_1 R_b(0) + Q_2 R_d(0)](\beta - a) + e^{-kL}[-Q_3 + a(1 + Q_1)]R_b(0) + e^{-k'L}[-Q_4 + a(1 + Q_2)]R_d(0)\}/\{e^{\alpha L}(1/\beta - a) - e^{-\alpha L}(\beta - a)\} \quad [7f]$$

$$C_2 = -\{C_1 + Q_1 R_b(0) + Q_2 R_d(0)\} \quad [7g]$$

$$C_3 = C_1/\beta$$
$$C_4 = C_2\beta \quad [7h]$$

Thermal infrared (longwave radiation)

As for the diffuse radiation, the longwave radiation coming from a point of the sky is also assumed to penetrate the canopy according to equation [1]. For integration over the entire hemisphere, the following 2 luminance distributions will be tested:

1) constant luminance:

$$N_l(\beta) = N_l(\pi/2) \quad \text{for any } \beta \quad [8a]$$

2) experimental distribution established on a clear summer day by radiothermometry (Berbigier and Lagouarde, unpublished results):

$$N_l(\beta) = N_l(\pi/2)\,(1.56 - 0.56\sin\beta) \quad [8b]$$

where $N_l(x)$ is the longwave luminance of any point of the sky with angular elevation x.

The numerical integration is made in the same way as for sky diffuse radiation. The results fit closely, for above luminance distributions, the following equations:

Constant luminance

$$R_l(\lambda)/R_l(0) = \exp(-0.548\lambda + 0.0177\lambda^2) \quad [9a]$$

Measured distribution

$$R'_l(\lambda)/R_l(0) = \exp(-0.583\lambda + 0.0215\lambda^2) \quad [9b]$$

where $R_l(\lambda)$ (W m^{-2}) is the longwave flux density of the sky that is not intercepted at LAI = λ inside the canopy.

As the absorptance of the leaves is nearly 1 in the thermal IR, the rescattered radiation is negligible.

The thermal emission of the canopy and understorey must be taken into account. Let:

Constant luminance

$$F = R_l(L)/R_l(0) = R_l(L)/(\sigma T_{sk}^4) \quad [10a]$$

(σ = 5.674 x 10^{-8} SI units, Stephan constant; T_{sk}: radiative sky temperature, K).

Measured distribution

$$F' = R'_l(L)/R_l(0) \quad [10b]$$

If the sky longwave luminance is constant, F may be considered as the horizontal projection of the 'holes' in the canopy, according to the directions of the longwave radiation passing through each 'hole'. The parts of the sky vault masked by foliage elements have a longwave luminance depend-

ing on their absolute temperature; their horizontal projection is $1 - F$. On the other hand, a proportion $1 - F$ of the radiation emitted by the ground will be intercepted by the canopy. Since the temperatures of the understorey, the different canopy elements and the air at the same levels (T_a, K) are nearly equal, the balance of the exchanges between the canopy and the understorey is negligible. Therefore, for a variable sky longwave luminance, the net radiation under the canopy may be written as:

$$R_n(L) = (1 - a)R_s(L) + R'_l(L) - F\sigma T_a^4$$

$$R'_l(L) = F'R'_l(0) = F'\{R_n(0) + \sigma T_a^4 - R_s(0) + R_{\_}(0)\}$$

where $R_s(x) = R_b(x) + R_d(x)$ is the non-intercepted flux density of solar radiation at LAI = x and $R_n(x)$ is the net radiation at LAI = x, and where all flux densities have units of Wm^{-2}.

Then, with the 'constant' distribution (F' reduces to F), we have:

$$R_n(L) = (1 - a)R_s(L) + F\{R_n(0) - R_s(0) + R_{\_}(0)\} \quad [11a]$$

and with the 'variable' distribution:

$$R_n(L) = (1 - a)R_s(L) + F'\{R_n(0) + \sigma T_a^4 - R_s(0) + R_{\_}(0)\} - F\sigma T_a^4 \quad [11b]$$

It can be seen that, with the 'constant' model, the effect of temperature vanishes.

RESULTS

Optical properties of the needles

Figure 2 displays the spectral reflectance and transmittance of the needles (3 years altogether). The properties of the flat and convex faces are almost identical. The transmittance is very low in the PAR, but cannot be neglected in the near infrared (NIR).

As mentioned earlier, the mean reflectance and transmittance of needles are estimated by summing the product of spectral reflectance and transmittance by the spectral density of the incident beam radiation of a selected clear day, and dividing this sum by the sum of spectral densities. For a sunny day we find, over the waveband 400–700 nm (PAR):

$$\rho = 0.090 \qquad \tau = 0.014$$

and over the waveband 400–1100 nm (solar radiation):

$$\rho = 0.279 \qquad \tau = 0.118$$

Example of radiation balance of a sunny day

Figure 3 displays the daily variation of the radiation balance on a sunny day at summer solstice, above and under the pine crowns. The effect of rows on underneath solar ($R_s(L)$) and net ($R_n(L)$) radiation can be clearly seen: the central peak is observed when the sun is directly above the inter-row where the mobile sensors are located, and the other 2 correspond to the nearest inter-rows. Two hollows are observed when the sun is aligned with the nearest rows of crowns.

The daily variation of the underneath diffuse radiation is very regular, and not affected at all by the effect of rows.

Modelling solar radiation penetration

Although the sky diffuse radiation was not measured at the site on days 177 and 178, we decided to use the data acquired on

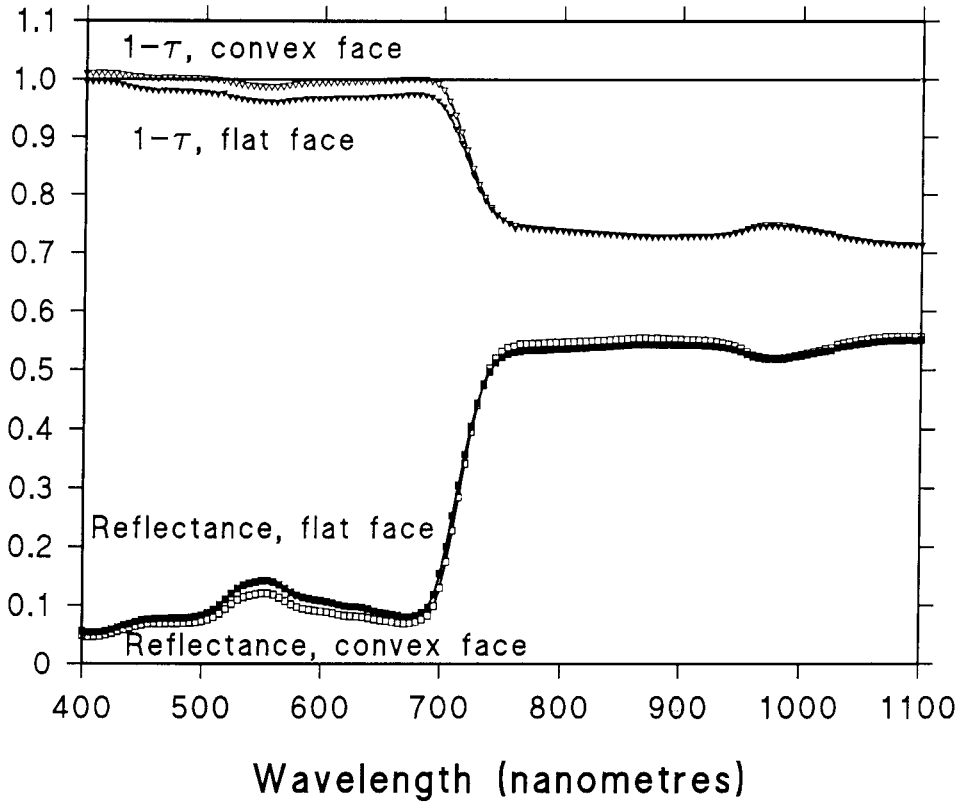

Fig 2. Spectral reflectance ρ and transmittance τ of the maritime pine needles.

these days to adjust the model, because at this time sun elevation was maximum.

Beam penetration

Although figure 3 shows that the hypothesis of a continuous canopy is only a rough approximation, it may still provide a good estimation of the mean radiation reaching the ground at the scale of the entire stand.

In figure 4, the mean hourly beam radiation that reached the understorey, as estimated by the difference between incident solar radiation and sky diffuse radiation (measured at Bordeaux on days 177 and 178), has been fitted to equation [1], and to a 2nd-order polynomial regression on the IST (international standard time) hour, which provides an unbiased least-square adjustment. It can be seen that the two adjustments give results very close to each other. The value of κL is found to be 0.992 ± 0.014. As the interpolated value of L is 3.1 (the standard deviation cannot be estimated objectively), it follows that:

$$\kappa = 0.32$$

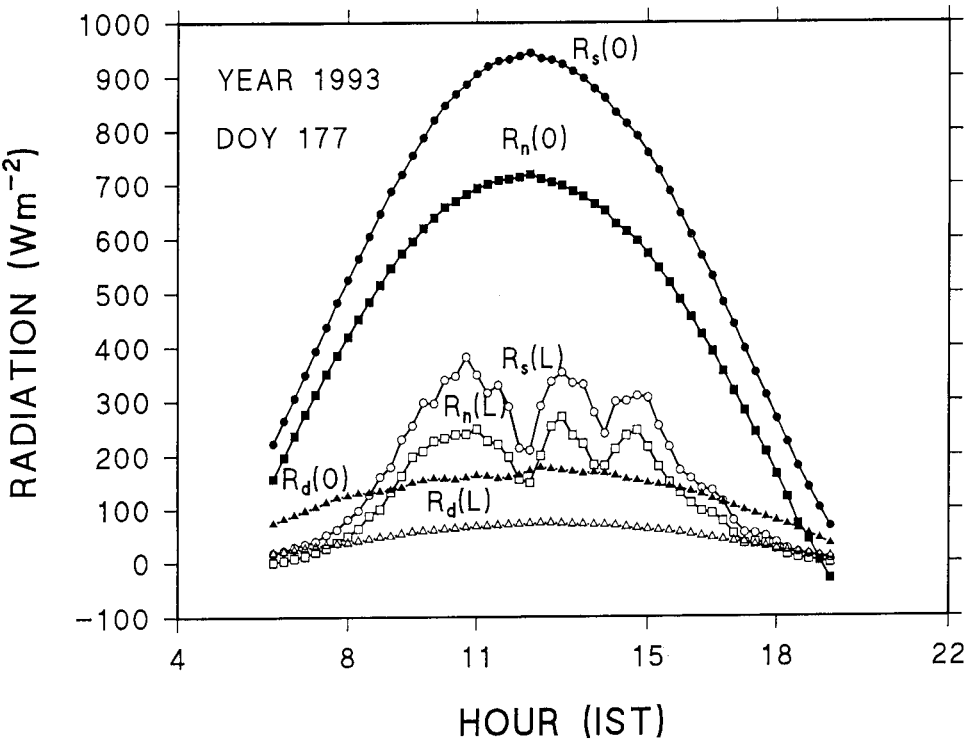

Fig 3. An example of radiative balance on a sunny day, above and under the canopy. Above the canopy: $R_s(0)$: solar (global) radiation; R_n (0): net radiation; $R_d(0)$: sky diffuse radiation. Under the canopy: $R_s(L)$: solar (global) radiation; $R_n(L)$: net radiation; $R_d(L)$: sky diffuse radiation.

Diffuse radiation

For simplicity, the non-intercepted sky diffuse radiation reaching the understorey is approximated in the manner discussed earlier:

$$R_d(L) = R_d(0) \exp(-0.467\ L)$$

which enables an analytical solution of the Kubelka–Munk equations. The downward rescattered radiation at the base of the canopy $R_+(L)$ and the upward rescattered radiation at its top $R_-(0)$ are then computed using equations [6] and [7].

As we could not make direct measurements of the albedo of the understorey, it was estimated at $a = 0.25$ for a grass height of about 0.7 m, as suggested by Monteith and Unsworth (1990).

Figure 5 shows the comparison between the measured upward radiation at the top of the canopy and the modelled $R_-(0)$. The agreement is very good. Moreover, it can be shown that the model is very insensitive to the variations in the albedo of the understorey.

For the downward diffuse radiation under the canopy, there is a small discrepancy between modelled $R_+(L) + R_d(0)\exp(-0.467\ L)$ and the measured diffuse radiation (fig 6). This was observed on day 177, whereas the agreement was much better

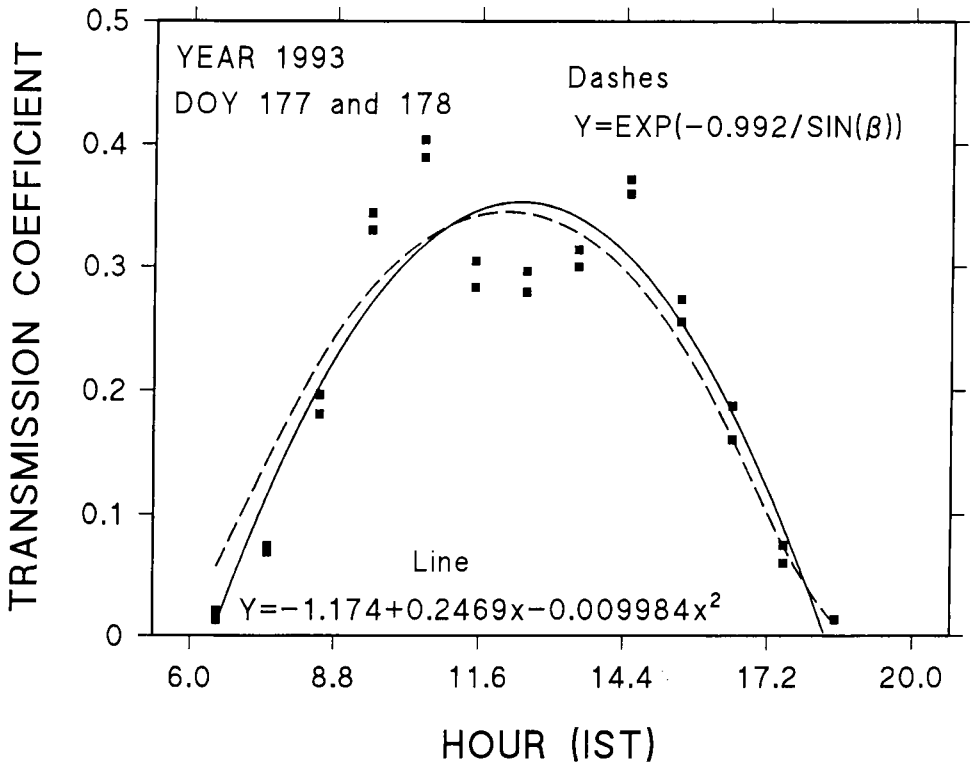

Fig 4. Least mean square adjustments of the measured transmission coefficient for direct radiation $R_b(L)/R_b(0)$ (squares) to: the penetration function $\exp-\kappa L/\sin\beta$ (dashes). Solar elevation β depends on time of the day. Relationship between model and data: $Y = 1.106X + 0.0270$, $R^2 = 0.876$; a 2nd-order ajustment on time of the day (line). Relationship between model and data: $Y = 0.999X + 0.0001$, $R^2 = 0.885$. The differences between slopes ($t = 1.33$, $df = 46$) and between zero-intercepts ($t = 1.38$, $df = 46$) are not significant at the 5% level.

on day 178. This may be due to the fact that the diffuse radiation of the sky was not measured on site. Whereas all the other radiative terms measured at the experimental site were essentially the same on days 177 and 178, the sky diffuse radiation measured at Bordeaux was different (maximum: 175 Wm^{-2} on day 177, 107 Wm^{-2} on day 178). On day 177, the sky was probably somewhat more cloudy at Bordeaux than at the site, inducing an overestimation of the diffuse radiation under the canopy by the model. This error did not exceed 10 Wm^{-2}.

Model validation

Late August early September 1993 (DOY 242 to 244)

This set of data was obtained at the same place under the same sunny conditions as for those measured earlier, with the exception that the sky diffuse radiation was measured on site (fig 7). LAI was estimated at 3.67.

The predictions agree well with the model. The downward scattered radiation

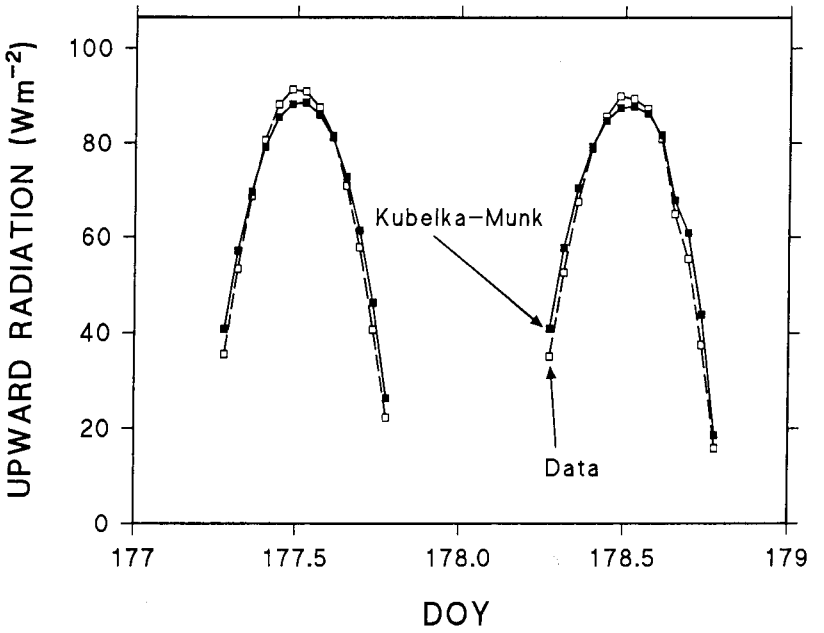

Fig 5. Upward rescattered radiation above the canopy (model *vs* data) on the 2 d used for model calibration (Year 1993, DOY 177 and 178).

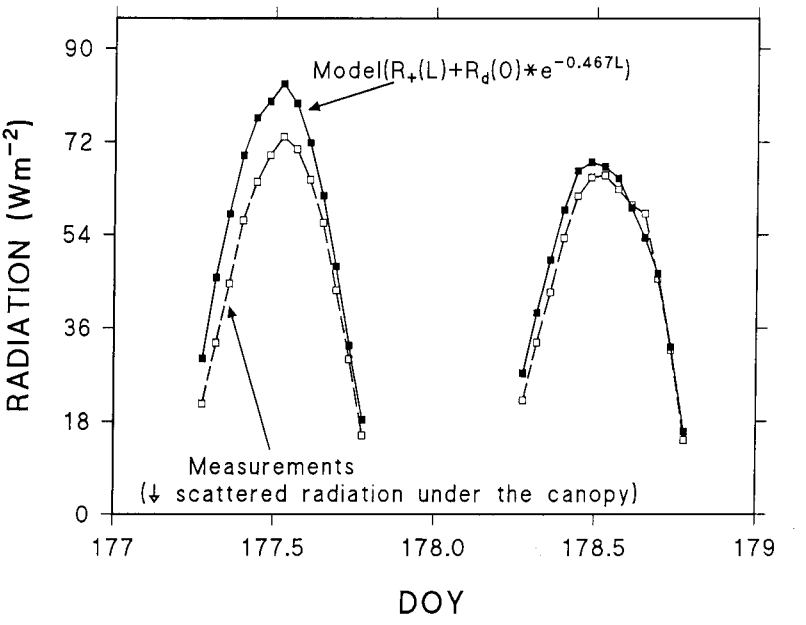

Fig 6. Downward scattered radiation under the canopy (model *vs* data) on the same days as figure 5.

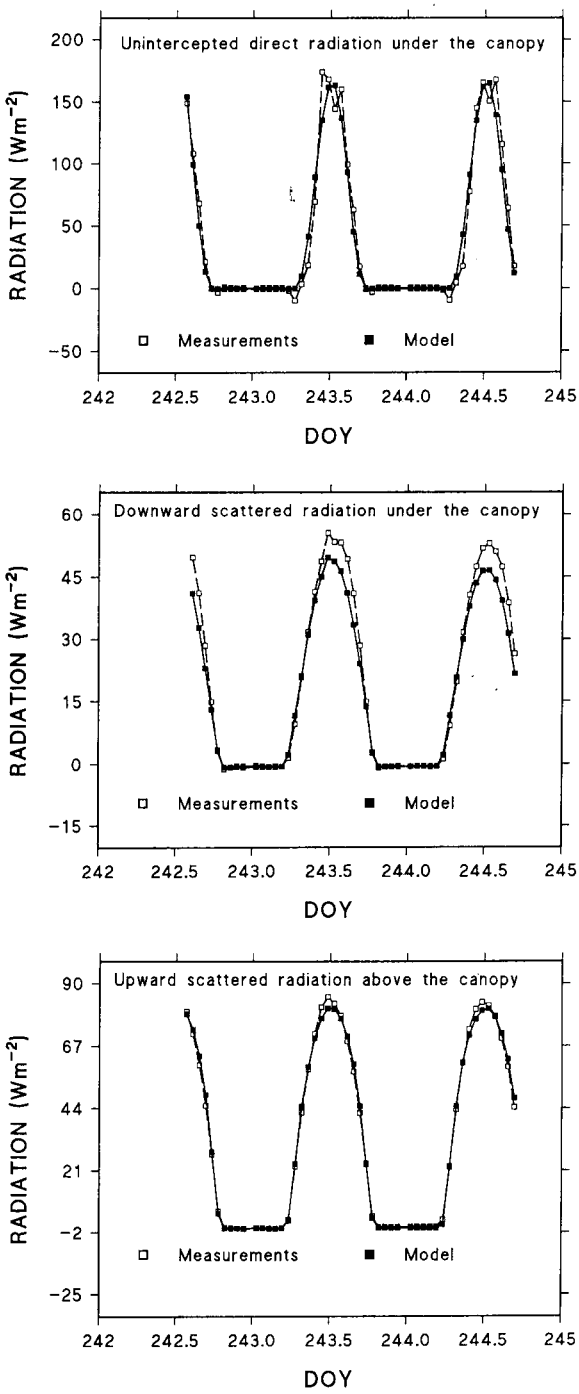

Fig 7. Model validation on another set of data (year 1993, DOY 242 to 245): a) non-intercepted direct radiation under the canopy; b) downward scattered radiation under the canopy; c) upward rescattered radiation above the canopy.

is somewhat underestimated (by 7 Wm^{-2} at maximum), in contrast to figure 6. The effect of rows has almost disappeared, as the maximum sun elevation decreased.

August 1991 (DOY 217 to 225)

In figure 8a and b, we show the measured and modelled hourly values of transmitted

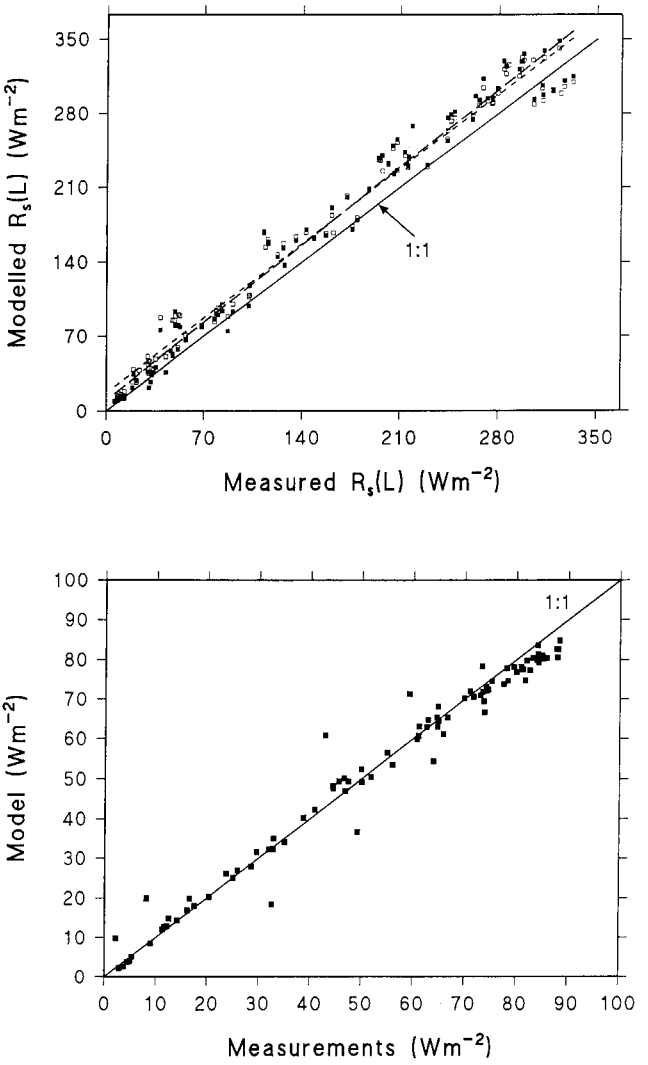

Fig 8. Model validation on another set of data (Year 1991, DOY 217 to 224): **a**) downward global radiation under the canopy. Full symbols: sky diffuse radiation measured at Bordeaux; open symbols: estimated by an empirical relationship (see text). The regression lines are confounded, both R^2 = 0.976. **b**) Upward rescattered radiation above the canopy (sky diffuse radiation measured at Bordeaux).

solar radiation under the canopy and reflected radiation above the canopy. As usual, the agreement is slightly worse for transmitted radiation, which was slightly overestimated by the model, but this discrepancy is less than 18 Wm^{-2}. The sky diffuse radiation was measured at Bordeaux. The LAI was 2.68.

We must stress the fact that the moving sensors were located at different places to 1993, and so the discrepancy between the stand and local LAI could be somewhat different. This could explain slight degradation of the agreement between model and data.

In figure 8a, we also display the results obtained using an empirical estimation of diffuse radiation currently used at Bordeaux (Valancogne, personal communication):

$$R_d(0)/R_s(0) = 1.41 - 1.7R_s(0)/\{1\ 390\sin(\beta)\}$$

This equation gives a poor estimation of $R_d(0)$ at the hourly level. On sunny days, it often underestimates the measurements made at Bordeaux by 100 Wm^{-2}. However, in any case, we find that the modelled value of $R_s(L)$ is almost unaffected.

Net radiation

Attempts were made to validate the model against the net radiation measurements of August 1992 and August–September 1993. Canopy LAIs were respectively 3.0 and 3.67. The longwave radiation balance under the canopy could be estimated in 1993 only when simultaneous measurements of both solar and net radiation were available.

In figure 9, the model is compared against measurement of net radiation under the canopy. The agreement is not very good. Moreover, the sign of the deviations differ for 1992 and 1993.

A more accurate analysis was possible in 1993 (fig 10). This showed that the choice of any of the 2 radiance distributions (equations [8a] and [8b]) had almost no effect on the longwave balance, so that the simplest model (equation [11a]), which does not require temperature measurements, could be used. We also conclude that the difference between the solar and net radiation balance under the canopy is too small to be measured accurately with thermopiles and net radiometers.

DISCUSSION

Interception of solar radiation by canopies has been widely studied. For conifers, the models vary from the totally empirical ones (Jarvis *et al,* 1976) to very sophisticated ones (see review by Berbigier, 1993). The main interest of the present work is to establish reliable experimental figures of radiation interception by maritime pines and to develop a simple semi-empirical model which allows us to avoid impractical radiation measurements under the tree crowns.

Beam interception

For horizontally continuous and homogeneous canopies (Sinoquet *et al,* 1993), the non-intercepted beam flux density at level λ is described by the function $y(\lambda) = y(0)\ \exp\{-G(\beta)\lambda/\sin\beta\}$, where $G(\beta)$ is the ratio between the horizontal projection of the surface of the elementary vegetation layer at level λ, and the surface itself. When the angular distribution of the leaves is random, $G(\beta) = 0.5$. Otherwise, for erectophile canopies, $G(\beta) < 0.5$ when $\beta > 33°$, and $G(\beta) > 0.5$ when $\beta < 33°$; the opposite applies for planophile canopies. For maritime pine, as the values of non-intercepted direct radiation at highest β angles, being the greatest, have more weight on the non-linear regression, the value $\kappa = 0.32 < 0.5$ implies that the canopy is erectophile.

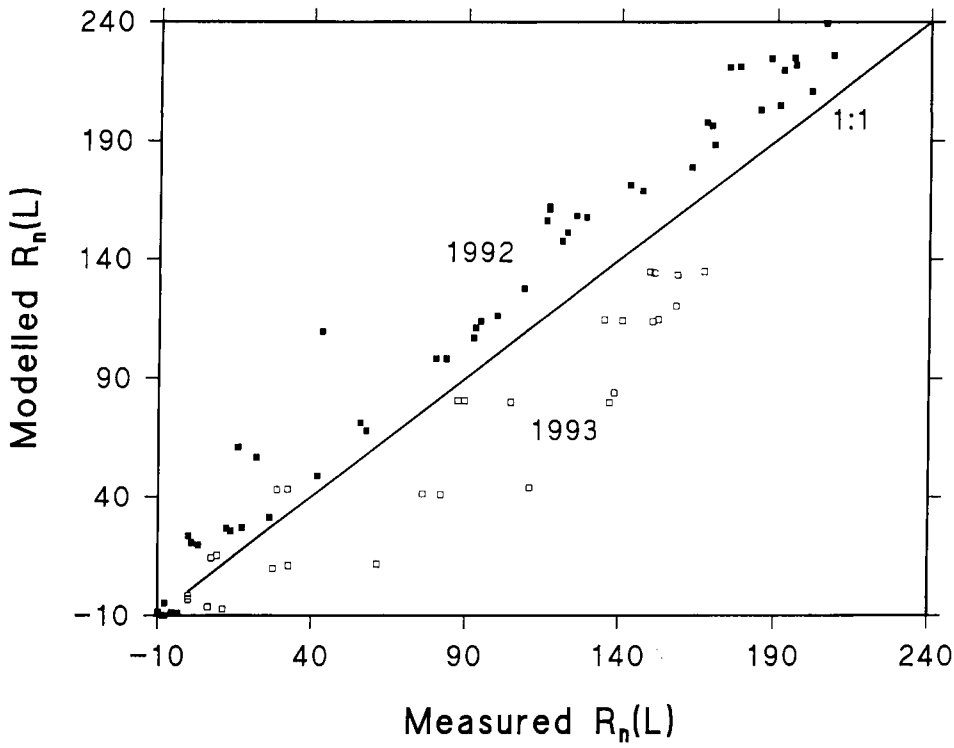

Fig 9. Modelled *vs* measured net radiation under the canopy (all data of years 1992 and 1993).

From several standard distribution functions (Campbell, 1986; De Wit, 1965), it is possible to use statistical adjustment to get a rough idea of an angular distribution of the foliage elements, assuming that it is the same for all layers. However, at the present, we prefer to wait for the experimental analysis of the canopy architecture of maritime pine, which is now being carried on by Dauzat and his colleagues (see Dauzat, 1993).

It was assumed that the canopy was continuous. Figures 3 and 4 show that, at a time scale of 1/4 to 1 h, this is clearly not the case at maximum sun elevations (almost 70° at summer solstice). However, comparison (fig 4) of the non-linear adjustment of $R_b(L)/R_b(0)$ to the function $\exp(-\kappa L/\sin\beta)$ with a second-order linear adjustement on time shows that

$$R_b(L) = R_b(0)\exp(-\kappa L/\sin\beta)$$

is an unbiased estimation of the mean beam radiation reaching the understorey.

Many models of discrete canopies can be found in the literature; for conifers, we can mention Kuuluvainen and Pukkala (1987), Pukkala *et al* (1991), who represent the tree crowns by cones, and Grace *et al* (1987), who simulate the different ages of needles with prolate ellipsoidal 'shells' included within each other. However, the 'continuous' model provides a very simple approach, which is accurate enough on the daily scale and quite convenient for estimating the evapotranspiration of the 2 vegetational layers.

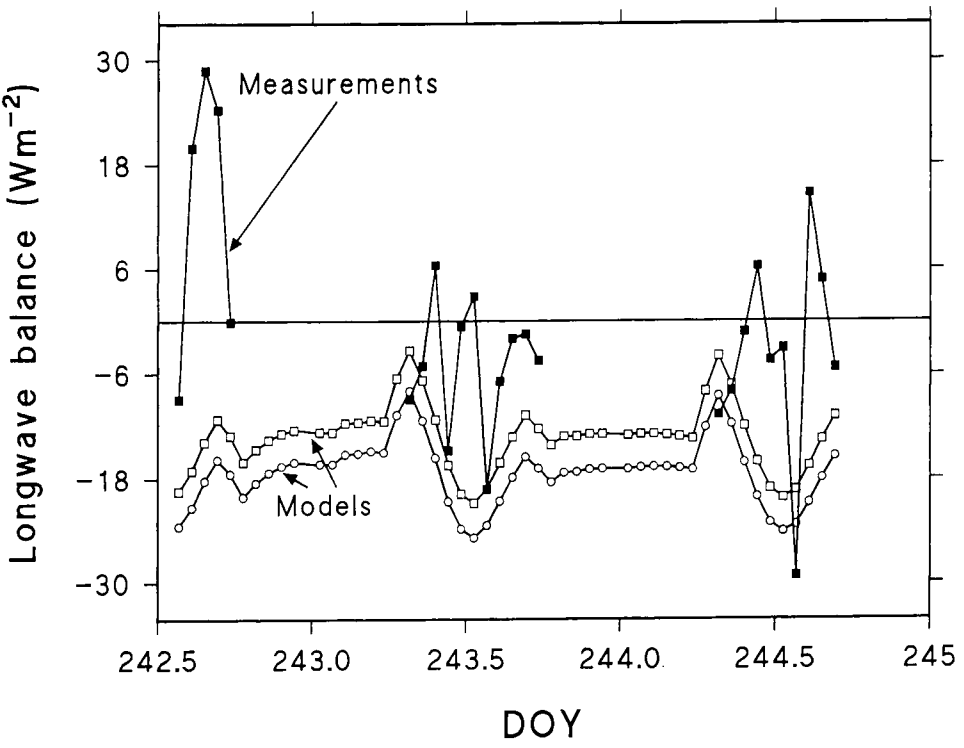

Fig 10. Modelled and measured longwave balance under the canopy. Open circles: equation [11a]. Open squares: equation [11b]. Full squares: measurements (see text).

With decreasing sun elevation, the row effect tends to vanish and by late August–early September (fig 7a), it is almost imperceptible on an hourly scale. In this case the expression $R_b(L) = R_b(0)\exp\{-\kappa L/\sin\beta\}$ with $\kappa = 0.32$, established for summer solstice, fits the data very well, and proves some validity for the non-linear adjustment shown in figure 4 for estimating the mean non-intercepted beam radiation.

Diffuse radiation

The penetration of the sky diffuse radiation follows the same laws as beam penetration, except for the problem of integrating the distribution of sky diffuse luminance over the sky vault. As outlined by Cowan (1968), the results of SOC and UOC (uniform overcast sky) models were almost the same, so that a constant sky luminance could have been used without appreciable error. The problem is quite different for clear skies. However, for these conditions, the proportion of diffuse radiation is less than 20%, and an error of estimation has little effect on the calculation of incoming solar radiation. The more cloudy it is, the more realistic become the SOC and UOC models.

When there is no available measurement of sky diffuse radiation, it can be estimated with a semi-empirical relationship where the ratio of diffuse to global radiation depends

linearly on the ratio of global radiation to extraterrestrial sun radiation, the coefficients being statistically adjusted for any particular place (Bonhomme, 1993). For the clear days of year 1991, this leads to a significant underestimation of diffuse radiation by about 100 Wm^{-2}. However, the modelled transmission of solar radiation is almost unaffected. This probably due to the fact that the transmission coefficient for diffuse radiation $R_d(L)/R_d(0)$ is more or less equal to the mean daily value of $R_b(L)/R_b(0)$ ($k = k' = 0.467$ for $\beta = 43°$).

Rediffused radiation

Models that take into account the rediffused solar radiation do so in the same way, by establishing the radiative balance of an elementary layer (or volume, for multidimensional ones) of the canopy (*eg,* Norman and Jarvis, 1975). Practically all assume that the rescattered radiation is Lambertian, despite the fact that the reflection by a leaf has a strong specular component (Breece and Holmes, 1971). This effect may be reduced by either needle curvature, and also by a nearly random spatial distribution of the needles.

The Kubelka–Munk model is a very simple one providing an analytical solution. However, assumptions of horizontal continuity and identical angle distribution of the needles within all the layers are questionable. This model may provide a good estimation of the spatial average of solar radiation under the canopy, but is probably a much poorer representation of radiation distribution within the canopy itself.

The precision of model estimation seems quite satisfactory, especially for the radiation scattered upwards above the canopy. The estimation of the diffuse radiation under the canopy is less precise: in 1993, an error of $\pm$ 10 Wm^{-2} can be observed depending on the period of measurement. In 1991, the model systematically underestimated the experimental data by 10–18 Wm^{-2}. One reason for these discrepancies could be that the stand LAI, as measured with the Demon system, did not correspond perfectly to the local LAI. Moreover, in 1991 the radiation measurements under the canopy were not made at the same place as in 1993.

Finally, the model shows that, for any kind of weather, from sunny to overcast, the downward rediffused radiation under the canopy is always about 15% of the non-intercepted radiation (beam + diffuse), so that it seems unnecessary to go into theoretical refinements about such a 2nd-order offset.

Net radiation

In the literature, the penetration of net radiation in canopies is mainly described by semi-empirical models. Existing models usually assume either an exponential attenuation:

$$R_n(\lambda) = R_n(0)\exp(-m\lambda)$$

(Cowan, 1968)

$$R_n(\lambda) = R_n(0)\exp(-m_1\lambda + m_2\lambda^2)$$

(Chartier, 1966),

where m, m_1, m_2 are empirical parameters. Unfortunately, because of the poor precision of the sensors located under the canopy, we could not validate our model. Discrepancies between modelled and measured $R_n(L)$ observed in 1992 and 1993 are significant (up to 50 Wm^{-2}) and opposite (fig 9). Comparing figure 8a and 9 shows that the problem comes from the net-radiometers, and more probably from the lower ones; it was not possible to calibrate these instruments *in situ* from the 4 radiative components that are too scattered under the canopy.

The poor precision of these instruments is well known (Field *et al,* 1992; Halldin and Lindroth, 1992) and is at best of the same order as the estimation of the longwave balance under the canopy, *ie* about 15–20 Wm^{-2}. Fortunately, the underneath longwave balance is so small that the model cannot lead to significant errors.

CONCLUSION

Despite its simplicity, this model provides a very good estimation of the mean solar (and probably net) radiation reaching the understorey, and an even better estimation of solar radiation reflected by the stand. However, many problems remain unresolved. Firstly, to what extent is the coefficient $\kappa = 0.32$ representative of this species? Measurements on stands of different ages and densities will be necessary to answer this question. When an experimental description of the needle distribution and tree architecture is available, it will be used to get a more deterministic representation of beam penetration taking into account the individual crowns. As it is, this work provides preliminary experimental data as well as an initial attempt at modelling the interception of radiation by maritime pine, a species covering some 10 000 km^2 in the south-west of France.

ACKNOWLEDGMENTS

The authors thank C Varlet-Grancher and his team for their help in determining the optical properties of the maritime pine needles, and KJ McAnemey for his help in establishing the English text.

REFERENCES

Berbigier P (1993) Radiative exchanges in forest canopies: the case of coniferous forests. *In: Crop Structure and Light Microclimate* (C Varlet-Grancher, R Bonhomme, H Sinoquet, eds) INRA, Versailles, France, 253-262

Berbigier P, Diawara A, Loustau D (1991) Étude microclimatique de l'effet de la sécheresse sur l'évaporation d'une plantation de pins maritimes et du sous-bois. *Ann Sci For* 22, 157-177

Bonhomme R (1993) The solar radiation; characterization and distribution in the canopy. *In: Crop Structure and Light Microclimate* (C Varlet-Grancher, R Bonhomme, H Sinoquet, eds), INRA, Versailles, France, 17-28

Bonhomme R, Varlet-Grancher C (1977) Application aux couverts végétaux des lois de rayonnement en milieu diffusant. I. Établissement des lois et vérification expérimentale. *Ann Agron* 28, 567-582

Bonnefond JM (1993) Étude d'un système mobile destiné à la mesure du rayonnement. Application à la mesure du rayonnement global et du rayonnement net sous un couvert de pins maritimes. *Cah Tech INRA* 30, 13-32

Breece HT, Holmes RA (1971) Bidirectional scattering characteristics of healthy green soybean and corn leaves *in vivo*. *Appl Optics* 10, 119-127

Campbell GS (1986) Extinction coefficients for radiation in plant canopies calculated using an ellipsoidal inclination angle distribution. *Agric For Meteorol* 36, 317-321

Chartier P (1966) Étude du microclimat lumineux dans la végétation. *Ann Agron* 17, 571-602

Cowan IR (1968) The interception and absorption in plant stands. *J Appl Ecol* 5, 367-379

Daughtry CST, Ranson KJ, Biehl LL (1989) A new technique to measure the spectral properties of conifer needles. *Remote Sens Environ* 27, 81-91

Dauzat J (1993) Simulated plants and radiative transfer simulations. *In: Crop Structure and Light Microclimate* (C Varlet-Grancher, R Bonhomme, H Sinoquet, eds), INRA, Versailles, France, 271-284

De Wit CT (1965) Photosynthesis of leaf canopies. Agricultural Research Report No 663, Center for Agricultural Publication and documentation, Wageningen, The Netherlands, 57 p

Diawara A (1990) Echanges d'énergie et de masse à l'intérieur et au-dessus d'une forêt de Pins des Landes, PhD thesis, Université de Clermont-Ferrand 2, 162 p

Diawara A, Loustau D, Berbigier P (1991) Comparison of two methods for estimating the evaporation of a *Pinus pinaster* (Ait) stand: sap flow and energy balance with sensible heat flux measurements by an eddy-covariance method. *Agric For Meteorol* 54, 49-66

Field RT, Fristchen LJ, Kanemasu ET *et al* (1992) Calibration, comparison, and correction of net radiation instruments used during FIFE. *J Geophys Res* 97, 18681-18695

Gash JHC, Shuttleworth WJ, Lloyd CR, André JC, Goutorbe JP, Gelpe J (1989) Micrometerological measurements in Les Landes forest during Hapex-Mobilhy. *Agric For Meteorol* 46, 131-147

Grace JC, Jarvis PG, Norman JM (1987) Modelling the interception of solar radiant energy in intensively managed stands. *N Z J For Sci* 17, 193-209

Granier A, Bobay V, Gash JC, Gelpe J, Saugier B, Sutleworth WJ (1990) Vapour flux density and transpiration rate comparisons in a stand of Maritime pines (*Pinus pinaster* Ait) in Les Landes forest. *Agric For Meteorol* 51, 309-319

Halldin S, Lindroth A (1992) Errors in net radiometry: comparison and evaluation of six radiometer designs. *J Atmos Oceanic Technol* 9, 762-783

Jarvis PG, James GB, Landsberg JJ (1976) Coniferous forests. *In: Vegetation and the Atmosphere,* Volume 2 (JL Monteith, ed) Academic Press, London, UK, 171-240

Kubelka P, Munk F (1931) Ein Beitrag zur Optik der Farbenstriche. *Zeits Furtechn Physick* 12, 593-601

Kuuluvainen T, Pukkala T (1987) Effect of crown shape and tree distribution on the spatial distribution of shade. *Agric For Meteorol* 40, 215-231

Lang ARG (1987) Simplified estimate of leaf area index from transmittance of the sun's beam. *Agric For Meteorol* 41, 179-186

Loustau D, Cochard H (1991) Utilisation d'une chambre de transpiration portable pour l'estimation de l'évapotranspiration d'un sous-bois de pin maritime à Molinie (*Molinia coerulaea* (L) Moench). *Ann Sci For* 48, 29-45

Loustau D, Granier A, El Hadj Moussa F (1990) Évolution saisonnière du flux de sève dans un peuplement de pins maritimes. *Ann Sci For* 21, 599-618

Monteith JL, Unsworth MH (1990) *Principles of Environmental Physics.* Edward Arnold, London, UK

Norman JM, Jarvis PG (1975) Photosynthesis in sitka spruce (*Picea sitchensis* (Bong) Carr). 5. Radiation penetration and a test case. *J Appl Ecol* 12, 839-878

Pukkala T, Becker P, Kuuluvainen T, Oker-Blom P (1991) Predicting spatial distribution of direct radiation below forest canopies. *Agric For Meteorol* 55, 295-307

Sinoquet H, Andrieu B (1993) The geometrical structure of plant canopies: characterization and direct measurement methods. *In: Crop Structure and Light Microclimate* (C Varlet-Grancher, R Bonhomme, H Sinoquet, eds), INRA, Versailles, France, 131-158

Sinoquet H, Varlet-Grancher C, Bonhomme R (1993) Modelling radiative transfer within homogeneous canopies: basic concepts. *In: Crop Structure and Light Microclimate* (C Varlet-Grancher, R Bonhomme, H Sinoquet, eds), INRA, Versailles, Fance, 207-228

Steven MD, Unsworth MH (1979) The diffuse irradiance of slopes uner cloudless skies. *Q JR Meteorol Soc* 105, 593-602

Steven MD, Unsworth MH (1980) The angular distribution and interception of diffuse solar radiation below overcast skies. *Q J R Meteorol* 106, 57-61